sustainability

MDPI

Article

Research on Hydraulic Support Attitude Monitoring Method Merging FBG Sensing Technology and AdaBoost Algorithm

Ningning Chen [1,2], Xinqiu Fang [1,2,*], Minfu Liang [1,2], Xiaomei Xue [3], Fan Zhang [1,2], Gang Wu [1,2] and Fukang Qiao [1,2]

[1] School of Mines, China University of Mining and Technology, Xuzhou 221116, China
[2] Research Center of Intelligent Mining, China University of Mining and Technology, Xuzhou 221116, China
[3] School of Information and Control Engineering, China University of Mining and Technology, Xuzhou 221116, China
* Correspondence: xinqiufang@cumt.edu.cn; Tel.: +86-(0516)-8359-0577

Abstract: The hydraulic support is the key equipment of surrounding rock support in a stope, and thus monitoring the attitude of the hydraulic support has an important guiding role in the support selection, operation control and rock pressure analysis of the working face. At present, attitude monitoring technology for hydraulic support mainly includes inertial measurement, contact measurement and visual measurement. Aiming at the technical defects of imperfect attitude perception models, incomplete perception parameters and the low decision-making ability of such systems, the fiber Bragg grating (FBG) pressure sensor and the FBG tilt sensor are developed independently by combining with FBG sensing theory. The pressure sensitivity of the FBG pressure sensor is 35.6 pm/MPa, and the angular sensitivity of the FBG tilt sensor is 31.3 pm/(°). Additionally, an information platform for FBG sensing monitoring for hydraulic support attitude is constructed based on. NET technology and C/S architecture. The information platform realizes real-time monitoring, data management, report management, production information management and data querying of hydraulic support attitude monitoring data. An AdaBoost neural network hydraulic support working resistance prediction model is established using MATLAB. The AdaBoost neural network algorithm successfully predicts the periodic pressure of the coal mining face by training with the sample data of the working resistance of the hydraulic support. The predicting accuracy is more than 95%.

Keywords: fiber Bragg grating (FBG); AdaBoost neural network algorithm; hydraulic support; attitude monitoring; intelligent monitoring

Citation: Chen, N.; Fang, X.; Liang, M.; Xue, X.; Zhang, F.; Wu, G.; Qiao, F. Research on Hydraulic Support Attitude Monitoring Method Merging FBG Sensing Technology and AdaBoost Algorithm. *Sustainability* **2023**, *15*, 2239. https://doi.org/10.3390/su15032239

Academic Editor: Constantin Chalioris

Received: 12 December 2022
Revised: 15 January 2023
Accepted: 20 January 2023
Published: 25 January 2023

1. Introduction

In recent years, the intelligent construction of coal mines has become the core technical issue for high-quality development in the coal industry. The core of coal mine intellectualization is to realize the intellectualization of a fully mechanized working face. However, the intelligent perception of the mining environment and the equipment operation state of the stope are the basis and prerequisites for achieving the intelligence of the fully mechanized working face [1–3]. The three pieces of mechanical supporting equipment of a fully mechanized working face are the shearer, scraper conveyor and hydraulic support. These three machines complete coal mining, coal transportation and face support through cooperative operation. The real-time, accurate and reliable perception and monitoring of the positioning and attitude information of the three machines, as an important prerequisite for realizing the remote control of equipment, has become a research hotspot in the field of intelligent mining in coal mines [4–6].

The hydraulic support is one of the important pieces of equipment for fully mechanized mining, which provides a safe and stable working space for personnel and equipment

in coal face production. In the process of moving forward with the working face, the hydraulic support undergoes adaptive changes in attitude such as lifting, lowering, looking up and looking down. However, the position and posture of the hydraulic support directly affect the supporting effect of the stope roof. The operating attitude information of the hydraulic support includes parameters such as attitude angle, working resistance, support height and hydraulic cylinder travel. The most representative hydraulic support control system in the world is the electro-hydraulic control system. The system has the functions of remote monitoring and control, which realizes the monitoring of the operating status of the hydraulic support and causes the fully mechanized working face to have the characteristics of automation.

At present, scholars, both domestic and foreign, have conducted much research on technologies related to hydraulic support attitude monitoring and have achieved certain results. Juárez-Ferreras et al. [7] have designed a fast solution program for the positional parameters of the main components of the hydraulic support and analyzed the mutual position relationship of the components during the lifting movement of the support. Reid et al. [8] have studied the three-dimensional positioning method of hydraulic support in a fully mechanized working face based on inertial navigation technology and have realized the straightening of a scraper conveyor based on hydraulic support attitude monitoring. Barczak et al. [9] have analyzed the kinematics and dynamics of hydraulic supports on longwall working faces. Vaze et al. [10] have established the attitude parameter expressions of each component of a shield hydraulic support and obtained the relationship between the telescopic length of the column and the inclination angle of the front bar and the top beam. Verma et al. [11] have established a pressure uncertainty estimation model of a hydraulic support by using a Bayesian neural network algorithm and designed a selection method for a hydraulic support for a long-wall working face through analyzing different influencing factors. Ge et al. [12] have established a kinematic model of the specific posture of a hydraulic support and carried out a kinematics simulation through its geometric model. Chen et al. [13] have proposed a measurement for coal mining height by installing a tilt sensor on a hydraulic support. The measurement accuracy was improved by using the Kalman filtering method to eliminate vibration noise. Wang et al. [14] have proposed a method for monitoring the memory attitude of a hydraulic support based on gray theory and verified its feasibility through experiments. Ren et al. [15] have established a hydraulic support attitude visual measurement model based on the motion mechanism of the support and have proposed a hydraulic support height and top beam posture angle measurement method based on depth vision. Meanwhile, the measurement system was built to provide a solution for hydraulic brace support height and top beam attitude angles. The above research provides important reference values for the establishment of a kinematics model of the specific posture of the hydraulic support, the construction of the posture parameter expression of the various components of the hydraulic support and the analysis of the error effect and the error model of the hydraulic support operating state.

At present, research on inertial measurement, contact measurement, visual measurement and other hydraulic support pose measurement technologies is still insufficient. The deficiencies are mainly reflected in the following aspects: the perception model of the hydraulic support operation attitude is not perfect, the parameter monitoring is not comprehensive, the monitoring accuracy of the hydraulic support attitude parameters is not high, and the monitoring data have not been deeply excavated and utilized.

Compared with conventional hydraulic support attitude monitoring sensor technology, the FBG sensor with a grating as the sensing element has the advantages of intrinsic safety, resistance against electromagnetic interference, low loss, good stability, high reliability and high precision. It is easy to form a quasi-distributed real-time online sensor network, which has a wide range of applications. By means of FBG sensing technology, multi-sensor information fusion and AdaBoost neural algorithm disaster prediction, the problem of accurate perception of hydraulic support attitude is solved. The research basis and

theoretical reference are provided for the realization of intelligent decision control of the hydraulic support and the inversion of the roof motion state.

2. Basic Theory

2.1. The Sensing Theory of the FBG

The fiber Bragg grating refers to a section of optical fiber that changes the core structure of germanium-doped fiber by means of strong ultraviolet light exposure and forms a phase grating with periodic refractive index changes and equidistant uniform distribution in the axial direction of the fiber core. The basic expression for the reflection wavelength of the FBG [16] is:

$$\lambda_B = 2n_{eff}\Lambda \tag{1}$$

where λ_B is the center wavelength of reflected light of the fiber grating, n_{eff} is the effective refractive index of the fiber core and Λ is the grating period.

Figure 1 details the FBG sensing principle. The light emitted by the broad-spectrum light source passes through the fiber grating, and the light meeting the grating wavelength condition of Equation (1) is reflected back to form reflected light. Other light is transmitted simultaneously. The reflected light is demodulated by a series of optical elements to obtain the peak of its center wavelength. When the FBG is used as the probe to sense the external temperature, pressure, stress and other physical quantities, the grating period Λ and effective refractive index n_{eff} of the grating part are changed, and the reflected wavelength will shift. The change in the reflected light wavelength follows certain rules with the change of external physical quantities, so the external temperature, pressure or stress can be deduced from monitoring the shift of the center wavelength of the FBG sensors.

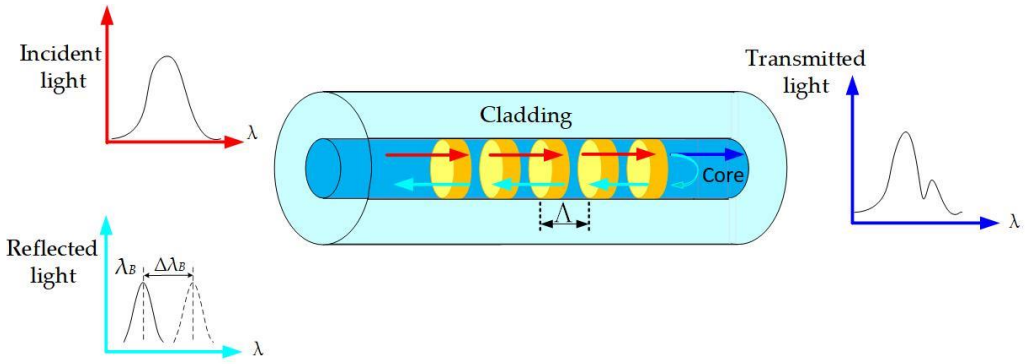

Figure 1. The fiber Bragg grating sensing principle.

When the optical fiber is only subjected to axial stress, the relationship between the center wavelength change of the reflected light and the axial strain on the grating is expressed by:

$$\frac{\Delta\lambda_B}{\lambda_B} = (1 - P_e)\varepsilon = K_\varepsilon\varepsilon \tag{2}$$

where $\Delta\lambda_B$ is the drift value of the center wavelength of the reflected light, ε is the axial strain of the fiber grating, P_e is the elasto-optical coefficient and K_ε is the sensitivity coefficient.

When the optical fiber is only affected by temperature, the relationship between the center wavelength change of the reflected light and the temperature is expressed by:

$$\frac{\Delta\lambda_B}{\lambda_B} = (\alpha + \zeta)\Delta T \tag{3}$$

where α is the thermal expansion coefficient of the optical fiber, ζ is the thermal-optic coefficient of the fiber and ΔT is temperature variation.

When the optical fiber is subjected to the double coupling of axial stress and temperature, the relationship between the center wavelength change of the reflected light and the independent variable is:

$$\frac{\Delta\lambda_B}{\lambda_B} = (1 - P_e)\varepsilon + (\alpha + \zeta)\Delta T \tag{4}$$

In order to eliminate the effect of temperature on the measurement results, an additional unstressed FBG sensor is often used for temperature compensation.

2.2. AdaBoost Neural Network Algorithm

The AdaBoost neural network algorithm is an important feature classification algorithm in machine learning which mainly solves classification and regression problems. At present, the algorithm has been applied to power system load monitoring and traffic volume forecasting, achieving appreciable prediction results. The specific training steps of AdaBoost algorithm are as follows [17–19]:

(1) Data collection $(x_i, y_i) i = 1, 2, 3, \ldots m$,

$$T = \{(x_1, y_1), (x_2, y_2), (x_3, y_3), \ldots (x_m, y_m)\}$$

(2) Initialize the weights of N samples. The initial sample weights $\omega_K(i)$ are uniformly distributed, $\omega_K(i) = 1/N$, where $\omega_K(i)$ is the weight of the sample in the Kth iteration and N is the number of samples in the training set.

(3) Under the weight of the training samples, the weak learner $h_i(x)$ is trained.

(4) The error e_i and average error $e_t = \frac{1}{N}\sum_{i=1}^{N} e_i$ of the weak learner under each sample are calculated.

(5) Update the sample weights $D_{t+1} = \frac{D_t(i)\eta_t^{-e_i}}{Z_t}$. The weights of weak learners are $R_t = \frac{1}{2}\ln(1/\eta_t)$, where $\eta_t = \frac{e_t}{1-e_t}$ and Z_t is the normalization factor for $\sum_{t=1}^{N} D_t(x_i) = 1$.

(6) The weak classifiers are calculated recursively until the number of iterations is t. Finally, the weak classifiers are combined according to their weights, that is, $f(x) = \sum_{t=1}^{T} R_t h_t(x)$.

(7) Through the action of the symbolic function *sign*, the strong predictor function is obtained as:

$$H_{final} = sign(f(x)) = sign\left(\sum_{t=1}^{T} R_t h_t(x)\right) \tag{5}$$

3. The FBG Intelligent Monitoring System for Hydraulic Support Attitude

3.1. The Coupling Model of the Hydraulic Support and Surrounding Rock in a Stope

The hydraulic support of the fully mechanized working face forms a dynamic, balanced support system relying on contacting the roof, coal wall and goaf gangue to form a safe and stable working space for coal mining [20]. The coupling model of the hydraulic support and the surrounding rock at the working face is shown in Figure 2.

After the coal seam is extracted, the coupling force of the hydraulic support and the surrounding rock is mainly composed of three parts. For part I, the load is generated by the weight of the residual top coal. For part II, the load is generated by the weight of the immediate roof. When the coal seam is mined out, the immediate roof cannot form a stable structure, which can be simplified to a cantilever force model. The weight of the immediate roof is directly or indirectly transferred to the support. For part III, the main roof transfers its self-weight to the hydraulic support in the form of torque through the immediate roof. The hydraulic support makes corresponding attitude changes according to the force and torque transmitted by the surrounding rock. By analyzing the coupling model of the hydraulic support and the surrounding rock, the support inclination and pressure

are taken as the research object of hydraulic support posture monitoring, which is of great significance for analyzing the mining pressure law of the working face and the dynamic change state of stress in the surrounding rock.

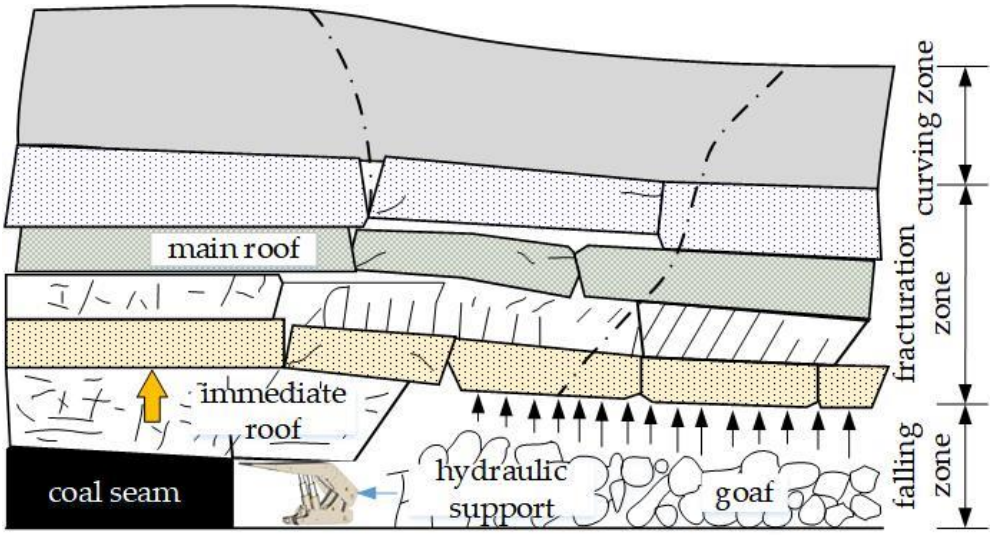

Figure 2. The coupling model of the hydraulic support and the surrounding rock.

3.2. The FBG Sensing System for Hydraulic Support Attitude

The attitude sensing system of the hydraulic support based on the FBG consists of the hardware equipment for FBG sensing monitoring and the software system. As shown in Figure 3, the hardware equipment for FBG sensing monitoring is mainly composed of the FBG sensors, the mine's intrinsically safe FBG demodulator, the intelligent controller, the electromagnetic actuator and other equipment. The FBG sensors and FBG demodulator are important components of the sensing system. The FBG sensors are connected in series or parallel to the main optical cable and then linked to the FBG demodulator. Finally, the FBG demodulator is connected to the underground ring network to form a quasi-distributed fiber-optic sensing monitoring network. The intelligent controller and electromagnetic actuator can drive, control and make decisions.

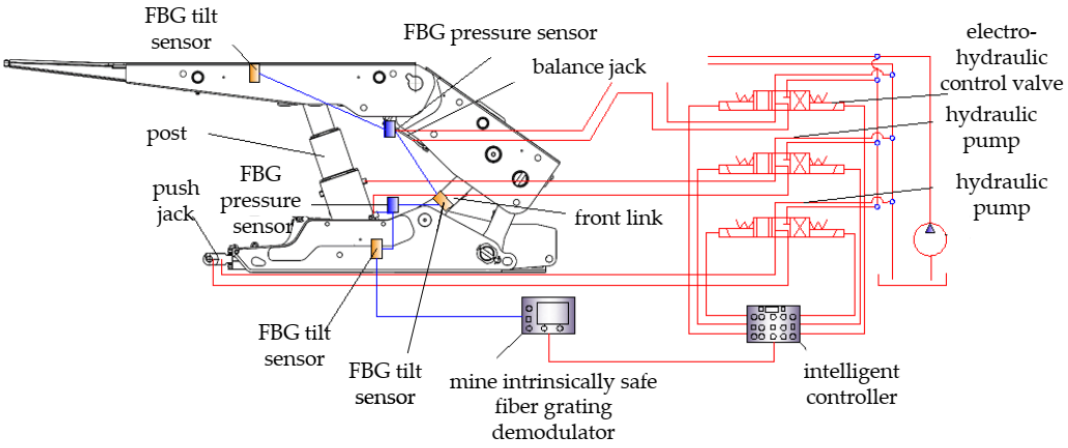

Figure 3. The hardware equipment composition of FBG sensing monitoring for hydraulic support attitude.

The network structure of the software system is shown in Figure 4. The information platform network, based on a C/S (client/server) architecture, consists of the application server, client and database. The underground FBG sensing information is connected with

the information platform network by the ethernet ring network, firewall, router and mine internal information network to realize data communication, real-time collection and analysis by the monitoring system.

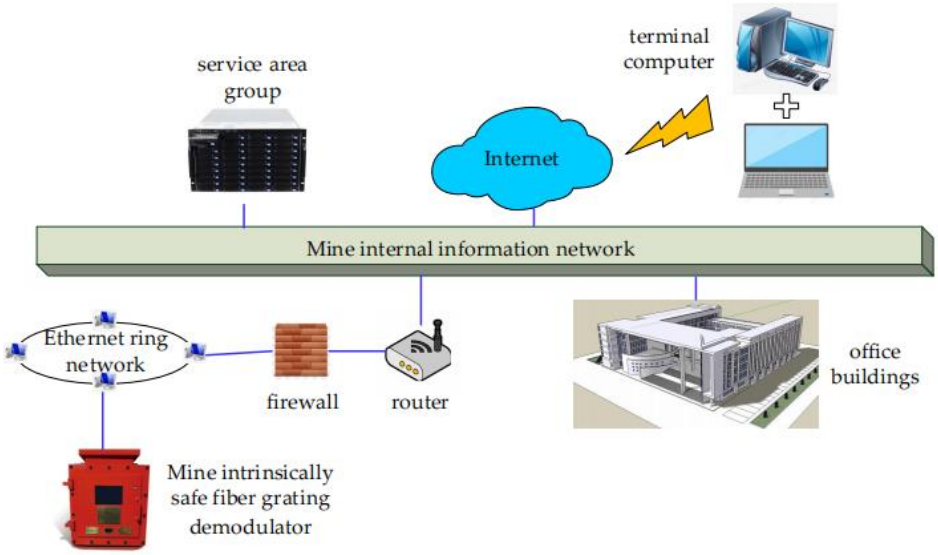

Figure 4. Network structure diagram of the software system.

3.2.1. The Hardware Equipment of FBG Sensing Monitoring

1. The FBG Pressure Sensor for Hydraulic Support

Figure 5 shows the structure and a photograph of an FBG pressure sensor for hydraulic support. Differently from a conventional support pressure sensor, the FBG pressure sensor takes an FBG manometer as the core component and uses FBG sensing technology to monitor the support oil pressure in real time. The FBG support pressure sensor is mainly composed of an FBG manometer, three-way valve, pressure gauge, pressure diaphragm, pressure guide interface and other components.

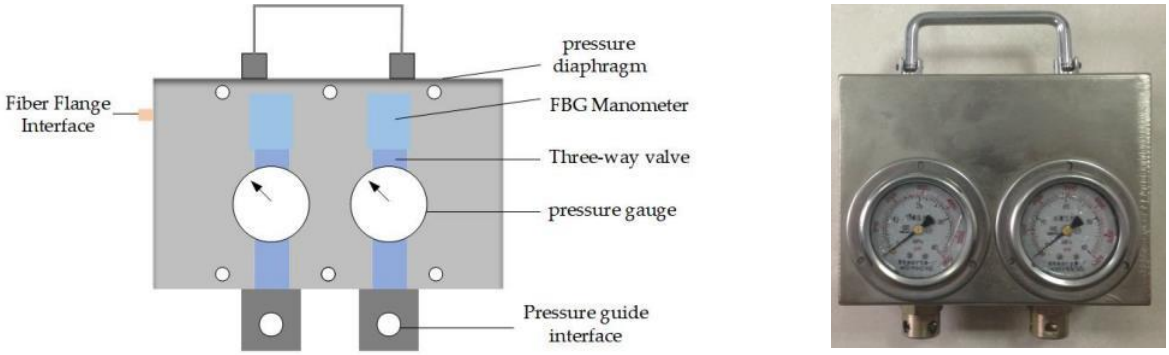

(**a**) (**b**)

Figure 5. The structure and a photograph of FBG pressure sensor. (**a**) Structure diagram; (**b**) Physical picture.

The pressure gauge, three-way valve and FBG manometer are located in the pressure diaphragm. The pressure guide interface is connected to the oil pipe. The FBG support pressure sensor is packaged in a membrane box with the following dimensions: length × width × thickness = 180 mm × 130 mm × 94 mm. The diameter of the pressure guide interface is 24 mm. The pressure gauge uses a YTN-60 stress-resistant pressure gauge with a range of 0 MPa~40 MPa and an accuracy grade of 2.5.

Figure 6 shows the structure of a diaphragm-connecting rod-type FBG manometer, which is mainly composed of a case, flat diaphragm, connecting rod, temperature-compensated FBG, pressure-sensitive FBG, fiber pigtail, fiber jacket and sealing element. The deflection deformation of the flat diaphragm under the action of environmental pressure will be transmitted to the pressure-sensitive FBG through the connecting rod. Subsequently, the pressure-sensitive FBG undergoes axial compression deformation, resulting in a corresponding shift of the center wavelength of the FBG under stress. The FBG pressure-sensing process involves the following steps: pressure change → elastic diaphragm deformation → FBG wavelength drift → the FBG demodulator solves the value of wavelength drift → solution of pressure value.

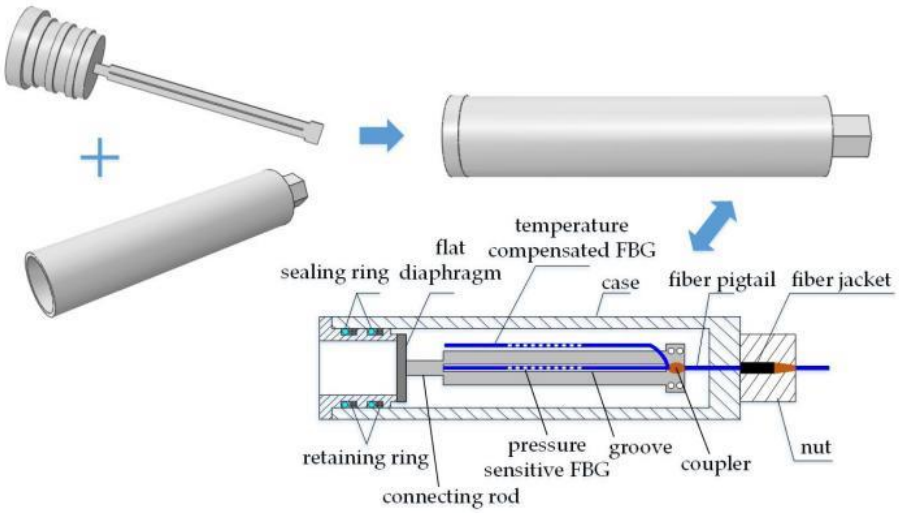

Figure 6. The structure diagram of FBG manometer.

The mathematical relationship between the variation of the FBG center wavelength and the pressure is as follows [21]:

$$P = \frac{16E_1Lh^3\left(1+\frac{3(1-\mu^2)R^2AE_f}{4\pi Eh^3L_f}\right)}{3(1-\mu^2)(1-P_e)R^4}\left(\frac{\Delta\lambda_P}{\lambda_P}-\frac{K_{T1}}{K_{T2}}\frac{\Delta\lambda_T}{\lambda_T}\right) \quad (6)$$

where E_1 is the elastic modulus of the diaphragm, h is the thickness of the diaphragm, L is the effective tensile length of the FBG, μ is the Poisson's ratio of the diaphragm, R is the distance of any point on the diaphragm from the center of the diaphragm, A is the sectional area of the connecting rod, L_f is the length of the connecting rod, K_{T1} and K_{T2} are temperature sensitivity of the pressure-sensitive FBG and the temperature-compensated FBG, respectively, λ_P is the initial wavelength of the pressure-sensitive FBG, $\Delta\lambda_P$ is the drift of the center wavelength of the pressure-sensitive FBG, λ_T is the initial wavelength of the temperature-compensated FBG and $\Delta\lambda_T$ is the drift of the center wavelength of the temperature-compensated FBG.

The FBG manometer is calibrated for pressure and temperature. In the pressure calibration experiment, an SSR-YBS-60TB pressure-loading device is used to load the FBG manometer from 0 to 20 MPa with an incremental gradient of 2 MPa, and it is then unloaded step by step. The FBG demodulator can record the center wavelength of the fiber grating during loading and unloading. The center wavelength of the pressure-sensitive grating decreases linearly with the increase of the pressure. The linearity is 0.9995, and the pressure sensitivity is 35.6 pm/MPa. In the temperature calibration experiment, the sensor is heated from 0 to 50 °C with a temperature gradient of 5 °C in an RTS-40 thermostat. The central wavelength of the pressure-sensitive grating increases linearly with the increase of the temperature. The linearity is 0.9993, and the temperature sensitivity is 10.62 pm/°C.

2. The FBG Tilt Sensor

Figure 7 shows a structural schematic of a double-cantilever-type FBG tilt sensor. As shown in Figure 7, the lower end of the pendulum is fixed to the heavy ball, and the upper end is hinged to the sensor body to ensure rotational freedom between the heavy ball and the pendulum. The tilt sensor includes isostrength cantilevers of the "L" type, namely cantilever beam 1 and cantilever beam 2. FBG1 is pasted onto the upper surface of cantilever beam 1, while FBG2 and FBG2′ are symmetrically stuck onto the left and right surfaces, respectively, of cantilever beam 2. The upper end of cantilever beam 2 is fixed to the sensor body, and the lower end is connected with the one end of cantilever beam 1. The other end of cantilever beam 1 is connected with the pendulum body.

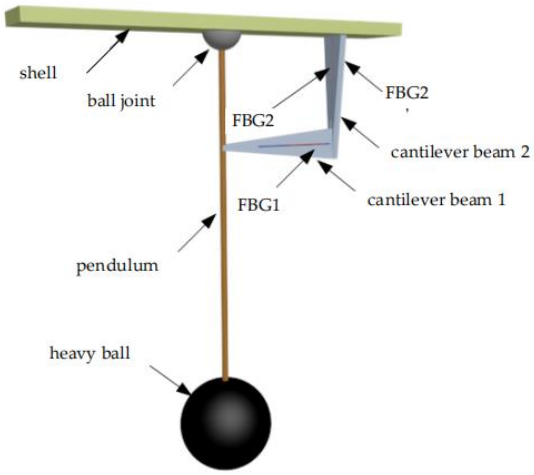

Figure 7. The structural schematic of the FBG tilt sensor.

As shown in Figure 8, when the sensor rotates in the X–Y plane, an axial force F_p in cantilever beam 1 is generated by the swinging action of the heavy ball and pendulum. Because the width-to-thickness ratio of the cantilever beam is large, the deformation of cantilever beam 1 is ignored. The axial force is transmitted to cantilever beam 2 through cantilever beam 1 and bends cantilever beam 2, causing wavelength changes for FBG2 and FBG2′. Finally, the angle wavelength conversion equation is used to measure the structural inclination monitoring. Similarly, inclination monitoring can be achieved in the Y–Z plane by solving the FBG1 wavelength variation on cantilever beam 1.

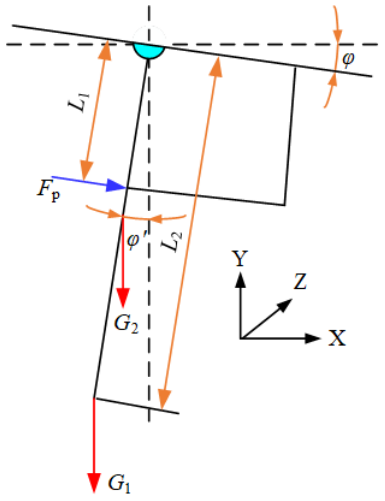

Figure 8. The mechanical model of the FBG tilt sensor.

The mathematical relationship between the inclination angle and the variation of the center wavelength is as follows [22]:

$$\Delta\lambda_B = \frac{6L_2\lambda_B}{E_2 b_0 h^2}\left(G_1 + \frac{G_2}{2}\right)(1 - P_e)\sin\varphi' = K_\varphi \sin\varphi' \quad (7)$$

where λ_B is the center wavelength of the FBG, $\Delta\lambda_B$ is the variation of the center wavelength of the FBG, L_2 is the length of the pendulum, G_1 is the self-weight of the heavy ball, G_2 is the self-weight of the pendulum, b_0 is the width of the upper end of cantilever beam 2, E_2 is the elastic modulus of the cantilever beam 2 and φ' is the deflection angle.

The FBG tilt sensor designed in this paper has good stability and accuracy in the range from $-45°$ to $45°$. The linear relationship between the angle and the center wavelength is good, with a linearity of 0.9988 and an angular sensitivity of 31.3 pm/(°). In practical applications, the elevation angle of the hydraulic support roof beam should be 0°~5°, and the limit range is $-5°$~$10°$.

3.2.2. The Software Information Platform of FBG Sensing Monitoring

The application server module of the FBG sensing monitoring software information platform is a Windows service program, which runs in the background of an industrial personal computer (IPC). The server-side program mainly completes two functions. One is to conduct TCP Modbus communication with the FBG demodulator and to store the monitoring data in a database system. The other is to provide application services for the client program. The thread flow chart of the server program is shown in Figure 9.

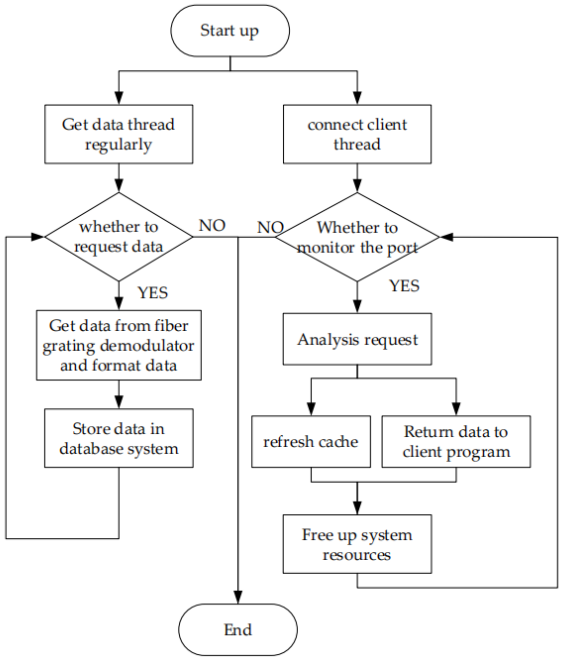

Figure 9. The thread flow chart of the server program.

The client of the software information platform is the terminal of the user for human–computer interaction in the information platform. The client program module is developed with the C/S model of. NET technology as the architecture. The structural diagram of the client program is shown in Figure 10. The client program uses the TCP socket protocol to communicate with the server program mutually by ethernet, thereby transferring the monitoring data from the database system to the data pool of the client program. The client program includes a real-time monitoring module, system management module, report module, production information module and data query module. The real-time monitoring module can read and write data to the data pool. The system management

module can add, modify and delete the basic information of the sensors. The production information module can add, modify and display the general production information of the application engineering system. The report module and the data query module implement the functions of report analysis and historical data querying, respectively.

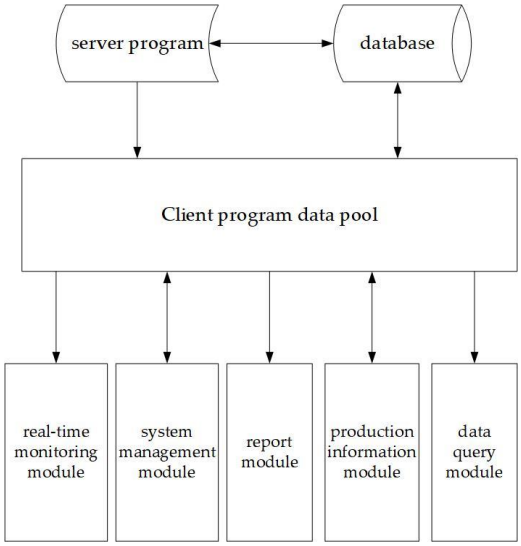

Figure 10. The structural diagram of the client program.

Figure 11 shows the interface of the software information platform. The buttons before and after the support model in the interface represent different FBG sensors, showing the sensor's running state through color changes. Green represents the sensor's normal operation, gray represents the sensor's failure, and red represents a warning message. When the user clicks on one of the buttons, the real-time monitoring value and basic information of the sensor are displayed in the information bar on the right side of the interface.

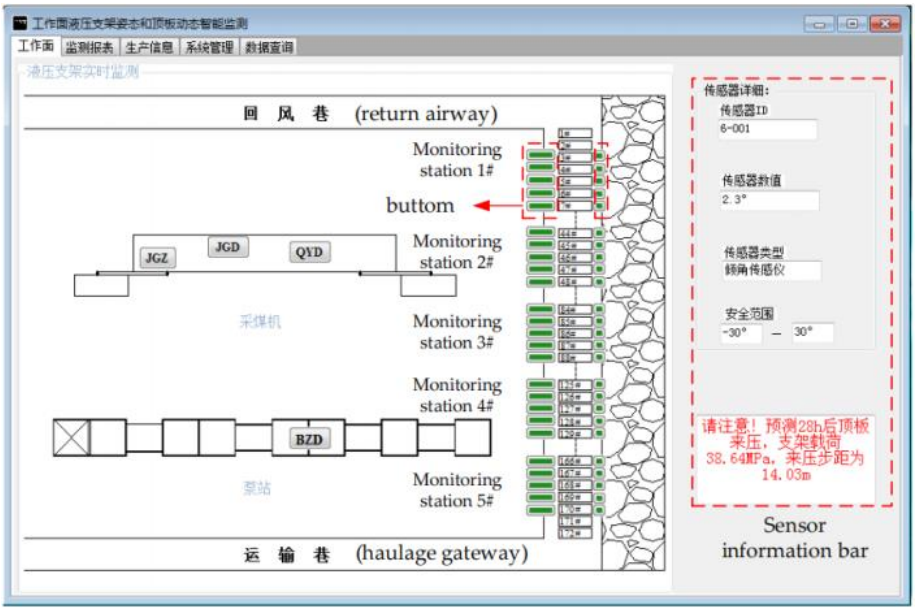

Figure 11. Interface of the software information platform.

The database module of the software information platform implements the functions of information management and data storage for the FBG sensors. The MySQL database

management system is used for the information management work. As shown in Table 1, the database module divides the information tables into two categories: logic control management information tables and data type tables.

Table 1. Information table of the database module.

Form Type	Description
Logic Control Management Information Table	The FBG sensing information list Correction information list Alarm information list
Data Type Table	Configuration information table of data correction module Monitoring data of the FBG tilt sensors Monitoring data of the FBG pressure gauges

4. Engineering Application

4.1. Project Overview

Working face 101 of the Longde coal mine is arranged in coal seam 1–1, with a recoverable thickness of 0.8~2.38 m, an average of 1.97 m and a burial depth of the coal seam of 130 m. Working face 101 is 300 m long, the recoverable length is 3596 m, and the dip angle is less than 1°. There are 170 hydraulic supports in the working face. The ZY10000/13/26D hydraulic support is selected for intermediate support, the ZYG10000/14/28D hydraulic support is selected for excessive support, and the ZT12000/16/32 hydraulic support is selected for end support.

4.2. The FBG Sensing System for Hydraulic Support Attitude

4.2.1. The FBG Sensing System

Electrical support pressure sensors were used in the Longde coal mine previously, with low accuracy and large errors. In order to promote the new technology, a hydraulic support attitude-sensing system based on FBG sensing technology is constructed. The FBG sensing system is mainly composed of the mine's intrinsically safe FBG demodulator, FBG tilt sensors, FBG manometers, an acquisition host, a light splitter, an optical fiber jumper and an armored optical cable used for signal transmission. The FBG demodulator and acquisition host are integrated into an explosion-proof shell and placed in a substation of the mining area. The FBG sensors are connected to the FBG demodulator through the optical fiber jumper and optical cable to form an FBG monitoring network. Then, through the ethernet ring providing network access to the information platform server and client, the real-time online monitoring of the inclination and pressure for the hydraulic supports is achieved.

4.2.2. Measuring Stations Arrangement

As shown in Figure 11, a total of five measuring stations are arranged in the working face. The first measuring station is arranged on the 3#~7# hydraulic supports, the second measuring station is arranged on the 44#~48# supports, the third measuring station is arranged on the 84#~88# brackets, the fourth measuring station is arranged on the 125#~129# supports, and the fifth measuring station is arranged on 166#~170# supports.

The FBG tilt sensors are installed on the top beam, front connecting rod and base of the hydraulic support, and the field installation diagram is shown in Figure 12. The FBG manometer is connected to the oil pipe drawn from the pressure hole of the hydraulic support auxiliary valve, and the field installation diagram is shown in Figure 13. The FBG tilt sensors and FBG manometers are arranged in series and parallel with the couplers and light splitters to form the monitoring units. The monitoring units are connected to the FBG demodulator through the optical fiber jumper and armored optical cable.

Figure 12. Field installation diagram of FBG tilt sensors.

Figure 13. Field installation diagram of FBG manometers.

4.3. Analysis of Monitoring Results

The monitoring data of five measuring stations for 73 days are exported. Figure 14 displays the variation curve of the top beam inclination angle and pressure of the 3# hydraulic support. The top beam inclination of the 3# hydraulic support is maintained within the range of 0.7°~4.2°. The inclination change range is small and basically stable, with small fluctuations in the middle, and there is no warning precursor. This shows that the top beam of the hydraulic support has good contact and support effects with the immediate roof in the mining process of the working face. On the other hand, the pitch angle of the top beam should be controlled within 0~5°, and the limit range is −5°~5°, so the inclination angle fluctuation of the 3# support top beam is in a reasonable range.

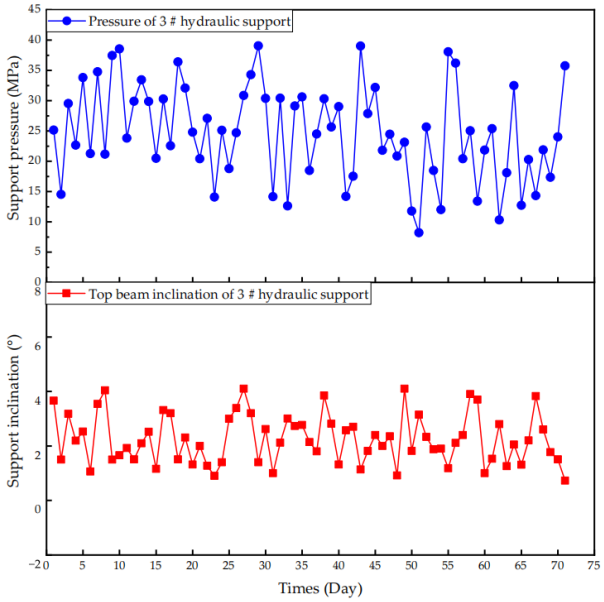

Figure 14. Field installation diagram of FBG manometer.

The support pressure fluctuates within the range of 8.2 to 39.05 MPa without a warning precursor. During the mining period, the working pressure of the support gradually increases due to the influence of the rock pressure, and the working pressure of the support gradually decreases in the process of lowering the support and moving forward.

Figure 15 shows the curve of the average working resistance of the hydraulic supports in the five monitoring stations of working face 101 for 73 days. The average working resistance of the hydraulic supports varies from 26.16 MPa to 39.76 MPa. During this period, the working resistance value of the hydraulic supports does not exceed the warning value, and the hydraulic supports are in normal working condition. The maximum values of the average working resistance of the supports at each station are 38.66 MPa, 39.77 MPa, 38.87 MPa, 39.33 MPa and 39.76 MPa. The minimum values are 29.5 MPa, 26.16 MPa, 29.23 MPa, 28.75 MPa and 29.9 MPa, respectively. The rated working resistance of the hydraulic supports is 10,000 kN (39.8 MPa), and the setting load is 8000 kN (31.5 MPa). Although the maximum working resistance of most supports does not exceed the rated working resistance, it is also close to 95% of the rated working resistance, which could indicate that the working face sometimes has severe pressure and a large dynamic load coefficient. In addition, the average working resistance of part of the hydraulic supports is less than the setting load. Therefore, it is necessary to check whether there are reasons such as insufficient pump station pressure, pipeline leakage or manual operation. In conclusion, the selection of hydraulic supports is reasonable and can satisfy the needs of field working resistance and roof support.

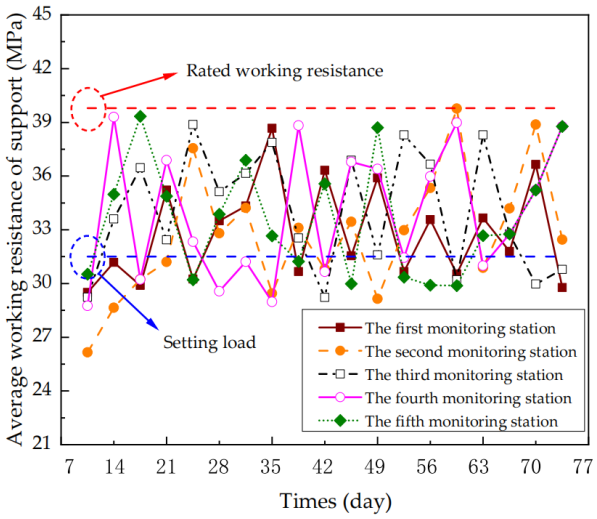

Figure 15. Change curve of the average support resistance with time.

Figure 16 shows the distribution law of the support working resistance along the inclination direction of the coal seam. It can be seen that the pressure distribution is large in the middle position and small at both ends. Among the supports, the 84#~88# supports have the maximum working resistance of 39.4 MPa, which is 98.99% of the rated working resistance. The hydraulic supports in the middle of the working face all reach more than 90% of the rated working resistance. The pressure distribution law of the hydraulic supports is consistent with the mine pressure distribution law of the working face, that is, the upper middle and lower middle parts of the working face are pressed first, then the air return roadway of the lower working face and finally the belt transportation roadway of the upper working face.

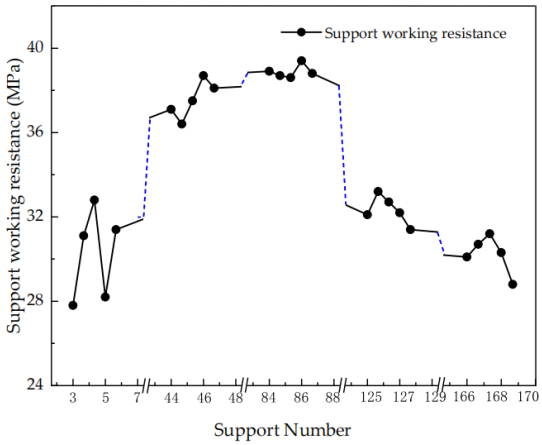

Figure 16. Support resistance distribution along the inclination direction of the coal seam.

4.4. AdaBoost Neural Network Algorithm Prediction

The AdaBoost neural network hydraulic support working resistance prediction model is established using MATLAB. The specific training process is as follows. (1) For the collected data, initialize the weights of N samples. (2) Find the weak function with the smallest error rate and calculate the weak classification function and error rate. (3) Combine the weak classifiers obtained from each training iteration into strong classifiers. The neural network fusion C language program trained by MATLAB is loaded into the server system to realize the monitoring function of the working face pressure.

In neural network intelligence learning, the larger the number of samples, the more accurate the prediction value. In total, 100 groups of hydraulic support pressure data

of working face 101 at a certain pressure from the monitoring system are selected. The 100 groups of data can reflect the roof pressure and are selected as data samples. Then, 90 groups of data are used as learning samples to train the neural network, and the remaining 10 groups of data are used as prediction samples to test the prediction accuracy of the network. The prediction results are shown in Figure 17.

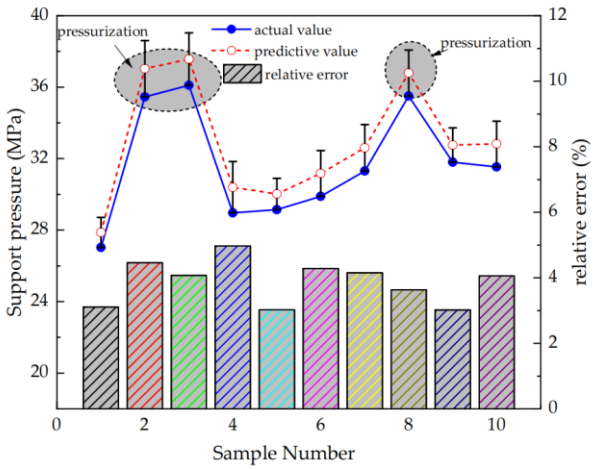

Figure 17. Forecast of pressure data for the working face.

The results show that the predicted and actual values of pressure during the periodic pressure have the same change trend, but the predicted value is greater than the actual value. The maximum relative error between the predicted value and the actual value is 4.97%, the minimum is 3.02%, and the accuracy is more than 95%. In conclusion, the calculation results of the AdaBoost neural network model have little error and high accuracy, which can meet the actual needs of engineering. Consequently, this proves the feasibility and effectiveness of intelligent monitoring and forecasting of working face pressure with an FBG monitoring system and AdaBoost neural network algorithm.

5. Conclusions

1. Based on the coupling model of a support and surrounding rock in a stope, the support inclination and pressure are identified as the research objects of support attitude sensing. In this paper, the FBG tilt sensor and FBG manometer are developed independently. In addition, an FBG sensing monitoring software information platform based on the C/S architecture model is developed.
2. A hydraulic support attitude FBG sensing system is constructed and tested on working face 101 of the Longde coal mine. The results show that the top beam inclination of the 3# hydraulic support is maintained within the range of 0.7°~4.2°, and the 3# hydraulic support pressure fluctuates within the range of 8.2 to 39.05 MPa without a warning precursor. The average working resistance of the hydraulic supports varies from 26.16 MPa to 39.76 MPa. During this period, the working resistance value of the hydraulic support does not exceed the warning value, and the hydraulic support is in normal working condition.
3. An AdaBoost neural network hydraulic support working resistance prediction model is established using MATLAB. The AdaBoost neural network algorithm successfully predicts the periodic pressure of the coal mining face by training with sample data of the working resistance of the hydraulic support. The results show that the prediction accuracy, judging from the difference between the predicted and actual values, is over 95%.

Author Contributions: Conceptualization, N.C. and X.F.; software, N.C.; validation, N.C. and X.F., F.Z., X.X., M.L., G.W. and F.Q.; data curation, N.C.; writing—original draft preparation, N.C. and F.Z.; writing—review and editing, N.C., X.F., F.Z., X.X., M.L., G.W. and F.Q.; project administration, N.C., X.F. and M.L.; funding acquisition, X.F., M.L. and G.W. All authors have read and agreed to the published version of the manuscript.

Funding: This work was supported by the National Natural Science Foundation of China (Nos. 51874276, 52004273 and 52104167), the Natural Science Foundation of Jiangsu Province (No. BK20200639), the China Postdoctoral Science Foundation (No. 2019M661992), the Fundamental Research Funds for the Central Universities (No. 2020ZDPY0209) and the Open Competition Mechanism to Select the Best Candidates Foundation of Shanxi Province (No. 20201101005).

Institutional Review Board Statement: Not applicable.

Informed Consent Statement: Not applicable.

Data Availability Statement: The data presented in this study can be made available on request from the corresponding author.

Acknowledgments: The authors would like to thank Huangbao Yan, Yutang Feng and Haiyang Lu for providing opportunities for engineering applications. The authors are also grateful to the editor and anonymous reviewers for their positive comments on the manuscript.

Conflicts of Interest: The authors declare no conflict of interest.

References

1. Wo, X.F.; Li, G.C.; Sun, Y.T.; Li, J.H.; Yang, S.; Hao, H.R. The Changing Tendency and Association Analysis of Intelligent Coal Mines in China: A Policy Text Mining Study. *Sustainability* **2022**, *14*, 11650. [CrossRef]
2. Li, M.; Zhang, X.P.; Mao, S.J.; Liu, Q.S. Study on deep mining safety control decision making system. In Proceedings of the International Conference on Mining Science & Technology, Xuzhou, China, 18–20 January 2009; pp. 377–384.
3. Wang, G.; Liu, F.; Pang, Y.; Ren, H.; Ma, Y. Coal mine intellectualization: The core technology of high quality development. *J. China Coal Soc.* **2019**, *44*, 349–357. [CrossRef]
4. Li, S.; Ren, H. Research status and development trend of position and posture measurement technology on hydraulic support, scraper conveyor, shearer in fully-mechanized mining face. *J. China Coal Soc.* **2020**, *48*, 219 226.
5. Negi, P.; Chakraborty, T.; Bhalla, S. Viability of electro-mechanical impedance technique for monitoring damage in rocks under cyclic loading. *Acta Geotech.* **2022**, *17*, 483–495.
6. Negi, P.; Chakraborty, T.; Bhalla, S. Damage Monitoring of Dry and Saturated Rocks Using Piezo Transducers. *J. Test. Eval.* **2017**, *45*, 169–181. [CrossRef]
7. Juárez-Ferreras, R.; González-Nicieza, C.; Menéndez-Díaz, A.; Álvarez-Vigil, A.E.; Álvarez-Fernández, M.I. Measurement and analysis of the roof pressure on hydraulic props in longwall. *Int. J. Coal Geol.* **2008**, *75*, 49–62. [CrossRef]
8. Reid, P.B.; Dunn, M.T.; Reid, D.C.; Palston, J.C. Real-world automation: New capabilities for underground longwall mining. In Proceedings of the Australasian Conference on Robotics and Automation, Brisbane, QLD, Australia, 6–8 December 2010.
9. Barczak, T.M.; Engineer, M. A retrospective assessment of longwall roof support with a focus on challenging accepted roof support concepts and design premises. In Proceedings of the 25th International Conference on Ground Control in Mining, Morgantown, WV, USA, 1–3 August 2006.
10. Vaze, J.; Jenkins, B.R.; Teng, J.; Tuteja, N.K. Soils fieldwork, analysis, and interpretation to support hydraulic and hydrodynamic modelling in the Murray floodplains. *Aust. J. Soil Res.* **2010**, *48*, 295–308. [CrossRef]
11. Verma, A.K.; Kishore, K.; Chatterjee, S. Prediction model of longwall powered support capacity using field monitored data of a longwall panel and uncertainty-based neural network. *Geotech. Geol. Eng.* **2016**, *34*, 2033–2052. [CrossRef]
12. Ge, X.; Xie, J.C.; Wang, X.W.; Liu, Y.; Shi, H.B. A virtual adjustment method and experimental study of the support attitude of hydraulic support groups in propulsion state. *Measurement* **2020**, *158*, 107743. [CrossRef]
13. Chen, D.F.; Li, S.B. Measurement of coal mining height based on hydraulic support structural angle. *J. China Coal Soc.* **2016**, *41*, 788–793.
14. Wang, Y.F.; Wang, X.W.; Xie, J.C.; Yang, Z.J. Memory attitude monitoring method for hydraulic support based on grey theory. *Ind. Mine Autom.* **2017**, *43*, 11–14.
15. Ren, H.W.; Li, S.S.; Zhao, G.R.; Zhang, K.X.; Du, M.; Zhou, J. Measurement method of support height and roof beam posture angles for working face hydraulic support based on depth vision. *J. Min. Saf. Eng.* **2022**, *39*, 72–81.
16. Wu, Z.X.; Wu, F. *Fiber Bragg Grating Sensing Principle and Application*, 1st ed.; Nation Defense Industry Press: Beijing, China, 2011; pp. 31–49.
17. Zhao, C.J. AdaBoost. In *Analysis of Machine Learning Electrostatic Algorithm: Based on OpenCV*, 1st ed.; Zhang, S., Ed.; Posts & Telecom Press: Beijing, China, 2018; pp. 120–141.

18. Yan, H.; Zhang, J.X.; Zhou, N.; Li, M. Application of hybrid artificial intelligence model to predict coal strength alteration during CO_2 geological sequestration in coal seams. *Sci. Total Environ.* **2020**, *711*, 135029. [CrossRef] [PubMed]
19. Yan, H.; Zhang, J.X.; Zhou, N.; Shi, P.; Dong, X.J. Coal permeability alteration prediction during CO_2 geological sequestration in coal seams: A novel hybrid artificial intelligence approach. *Geomech. Geophys. Geo-Energy Geo-Resour.* **2022**, *8*, 104. [CrossRef]
20. Zhang, K.; Li, Y.X.; Feng, L.; Meng, X.J.; Zhong, D.H.; Huang, L.S. Roof deformation characteristics and experimental verification of advanced coupling support system supporting roadway. *Energy Sci. Eng.* **2022**, *10*, 2397–2419. [CrossRef]
21. Liang, M.F.; Fang, X.Q.; Bai, H.L.; Xing, X.P.; Wu, G. Application of temperature compensation fiber Bragg grating pressure sensor for bolting quality monitoring. *J. China Coal Soc.* **2017**, *42*, 2826–2833.
22. Liang, M.F.; Fang, X.Q.; Li, S.; Wu, G.; Ma, M.; Zhang, Y.G. A fiber Bragg grating tilt sensor for posture monitoring of hydraulic supports in coal mine working face. *Measurement* **2019**, *138*, 305–313. [CrossRef]